Available online at www.sciencedirect.com

ScienceDirect

Nuclear and Particle Physics Proceedings 273–275 (2016) 1358–1363

www.elsevier.com/locate/nppp

Measurement of the CKM angle γ with $B_s^0 \to D_s^{\mp} K^{\pm}$ decays

Agnieszka Dziurda
on behalf of the LHCb Collaboration

Henryk Niewodniczanski Institute of Nuclear Physics PAS, Cracow, Poland

Abstract

This document reports the first measurements of the time-dependent CP violating observables in $B_s^0 \to D_s^{\mp} K^{\pm}$ decays. The measurements are performed using data corresponding to an integrated luminosity of 1 fb^{-1} collected in 2011 by the LHCb detector. The CP violating observables: $C_f = 0.53 \pm 0.25 \pm 0.04$, $A_f^{\Delta\Gamma} = 0.37 \pm 0.42 \pm 0.20$, $A_{\overline{f}}^{\Delta\Gamma} = 0.20 \pm 0.41 \pm 0.20$, $S_f = 1.09 \pm 0.33 \pm 0.08$, $S_{\overline{f}} = 0.36 \pm 0.34 \pm 0.08$ are found, where the uncertainties are statistical and systematic. Later, these observables are used to deterimine the CKM angle γ from $B_s^0 \to D_s^{\mp} K^{\pm}$ decays. A γ value of $(115^{+28}_{-43})^{\circ}$ modulo 180° at 68% CL is found, where the uncertainty contains both statistical and systematic components.

1. Introduction

In the Standard Model (SM) CP violation in weak interactions is described by a single, irreducible phase in the Cabibbo-Kobayashi-Maskawa (CKM) mixing matrix [1, 2]. The unitarity of the CKM matrix implies a set of relations among its elements V_{ij}, in particular the condition:

$$V_{ud}V_{ub}^* + V_{cd}V_{cb}^* + V_{td}V_{tb}^* = 0, \qquad (1)$$

which can be presented in the complex plane as a Unitarity Triangle (UT). Overconstraining the unitarity triangle with precise measurements of all its sides and angles is therefore a test of the SM.

Time-dependent analyses of $B_s^0 \to D_s^{\mp} K^{\pm}$ decays[1] are sensitive to the least-well measured angle of the CKM matrix, the angle γ equal to $\arg(-V_{ud}V_{ub}^*/V_{cd}V_{cb}^*)$. CP violation in such decays comes from the interference of mixing and decay amplitudes [3]. The importance of this measurement lies in the fact that $B_s^0 \to D_s^{\mp} K^{\pm}$ is a pure tree-level decay, and is therefore a standard measurement to which other observables sensitive to physics beyond the Standard Model can be compared.

Due to the interference between mixing and decay amplitudes, the CP violating observables in these decays are functions of a combination of γ and the mixing phase $-2\beta_s$: $\gamma - 2\beta_s$, where $\beta_s \equiv \arg(-V_{ts}V_{tb}^*/V_{cs}V_{cb}^*)$ in the B_s^0 system. A measurement of these physical observables can be interpreted in terms of γ or β_s by using an independent measurement of the other parameter as input.

The time-dependent decay rates of the initially produced flavour eigenstates $|B_s^0(t=0)\rangle$ and $|\overline{B}_s^0(t=0)\rangle$ are given by:

$$\frac{d\Gamma_{B_s^0 \to f}(t)}{dt} = \frac{1}{2}|A_f|^2(1+|\lambda_f|^2)e^{-\Gamma_s t}[cosh(\tfrac{\Delta\Gamma_s t}{2}) + A_f^{\Delta\Gamma} sinh(\tfrac{\Delta\Gamma_s t}{2}) + C_f cos(\Delta m_s t) - S_f sin(\Delta m_s t)], \qquad (2)$$

$$\frac{d\Gamma_{\overline{B}_s^0 \to f}(t)}{dt} = \frac{1}{2}|A_f|^2(1+|\lambda_f|^2)e^{-\Gamma_s t}[cosh(\tfrac{\Delta\Gamma_s t}{2}) + A_f^{\Delta\Gamma} sinh(\tfrac{\Delta\Gamma_s t}{2}) - C_f cos(\Delta m_s t) + S_f sin(\Delta m_s t)]. \qquad (3)$$

[1] Inclusion of charge conjugate modes is implied except where explicitly stated.

http://dx.doi.org/10.1016/j.nuclphysbps.2015.09.219

The CP observables are related to the magnitude of the amplitude ratio $r_{D_sK} \equiv |A(\overline{B}_s^0 \to D_s^- K^+)/A(B_s^0 \to D_s^- K^+)|$, the strong phase difference δ, and the weak phase difference $\gamma - 2\beta_s$ by the following equations:

$$\begin{gathered} C_f = \frac{1-r_{D_sK}^2}{1+r_{D_sK}^2}, \\ A_f^{\Delta\Gamma} = \frac{-2r_{D_sK}\cos(\delta-(\gamma-2\beta_s))}{1+r_{D_sK}^2}, A_{\overline{f}}^{\Delta\Gamma} = \frac{-2r_{D_sK}\cos(\delta+(\gamma-2\beta_s))}{1+r_{D_sK}^2}, \\ S_f = \frac{2r_{D_sK}\sin(\delta-(\gamma-2\beta_s))}{1+r_{D_sK}^2}, S_{\overline{f}} = \frac{-2r_{D_sK}\sin(\delta+(\gamma-2\beta_s))}{1+r_{D_sK}^2}. \end{gathered} \quad (4)$$

2. Event selection

The analysis is based on a sample of proton-proton collisions data corresponding to an integrated luminosity of 1 fb^{-1} collected by LHCb detector. The full description of detector can be found in [4].

In the measurement three different D_s^- final states are considered: $D_s^- \to K^-K^+\pi^-$, $D_s^- \to K^-\pi^+\pi^-$, and $D_s^- \to \pi^-\pi^+\pi^-$. In addition, $D_s^- \to K^-K^+\pi^-$ is split depending on the position in the Dalitz plane, into: $D_s^- \to \phi\pi^-$, $D_s^- \to K^{*0}K^-$ and the remaining decays. These D_s^- candidates are subsequently combined with a fourth particle, referred to as the "companion", to form $B_s^0 \to D_s^\mp K^\pm$ and $B_s^0 \to D_s^-\pi^+$ candidates.

For the optimisation of the selection and for studying and constraining physics backgrounds to the $B_s^0 \to D_s^\mp K^\pm$ decay the flavour-specific Cabibbo-favoured decay mode $B_s^0 \to D_s^-\pi^+$ is used as a control channel.

The different final states are distinguished by using PID information from RICH detector. This selection is necessarily different for each D_s^- decay mode and strongly suppresses cross-feed and peaking backgrounds from other misidentified decays of b-hadrons to c-hadrons.

In addition, the B_s^0 and D_s^- candidates are required to be within $m(B_s^0) \in [5300, 5800] MeV/c^2$ and $m(D_s^-) \in [1930, 2015] MeV/c^2$, respectively.

3. Multivariate fit to $B_s^0 \to D_s^\mp K^\pm$ and $B_s^0 \to D_s^-\pi^+$

The determination of the signal and background component yields in the samples of $B_s^0 \to D_s^\mp K^\pm$ and $B_s^0 \to D_s^-\pi^+$ candidates is done using a simultaneous extended maximum likelihood fit, where the fitting variables are: the B_s^0 mass, the D_s^- mass, and the log-likelihood difference $L(K/\pi)$ between the pion and kaon hypotheses for the companion particle.

The decay modes $B^0 \to D^-\pi^+$, $B^0 \to D_s^-\pi^+$, $\overline{\Lambda}_b^0 \to \overline{\Lambda}_c^-\pi^+$, $B_s^0 \to D_s^\mp K^\pm$, and $B_s^0 \to D_s^{*-}\pi^+$ are backgrounds to $B_s^0 \to D_s^-\pi^+$, while $B_s^0 \to D_s^-\pi^+$, $B_s^0 \to D_s^{*-}\pi^+$, $B_s^0 \to D_s^-\rho^+$, $B^0 \to D_s^-\pi^+$, $B^0 \to D^-K^+$, $B^0 \to D^-\pi^+$, $\overline{\Lambda}_b^0 \to \overline{\Lambda}_c^-K^+$, $\overline{\Lambda}_b^0 \to \overline{\Lambda}_c^-\pi^+$, and $\Lambda_b^0 \to D_s^{(*)-}p$ are backgrounds to $B_s^0 \to D_s^\mp K^\pm$.

Correlations between the fitting variables are measured to be small in simulation, so the multivariate fit can be built from the product of the signal and background PDFs, which then are added for each D_s^- final state. Almost all background yields are left free to float, however the backgrounds whose yields are below 2% of the signal yield are fixed from known branching fractions and relative efficiencies measured using simulated events. The multivariate fit results in a signal yield of 28 260 ± 180 $B_s^0 \to D_s^-\pi^+$ and 1770 ± 50 $B_s^0 \to D_s^\mp K^\pm$ decays, shown in Fig. 1 and Fig. 2, respectively. An effective purity of 85% for $B_s^0 \to D_s^-\pi^+$ and 74% for $B_s^0 \to D_s^\mp K^\pm$ are measured. The multivariate fit is checked for biases using large samples of data-like pseudoexperiments, and none are found.

4. Decay time fit to $B_s^0 \to D_s^\mp K^\pm$ and $B_s^0 \to D_s^-\pi^+$

4.1. Flavour tagging

The measurement requires the tagging of the initial flavour of the decaying B_s^0 meson. At the LHCb experiment, two types of flavour-tagging algorithms are in use [5]. The opposite side (OS) tagging algorithms rely on the pair production of b and $\bar{b}$ quarks and infer the flavour of a given signal beauty meson from the identification of the flavour of the other b-hadron. The same side kaon (SSK) tagger on the other hand searches for an additional charged kaon accompanying the fragmentation of the signal B_s^0 or $\overline{B}_s^0$. Due to tracks from the underlying event, particle misidentifications, or flavour oscillations of neutral B mesons each of these algorithms has an intrinsic mistag rate ω = (wrong tags)/(all tags).

The mistag probability, η, is predicted for each B_s^0 candidate using a neural network trained on simulated events. The estimated η is treated as a per-candidate variable in the fit. Due to variations in the properties of tagging tracks for different channels, the predicted mistag probability η has to be calibrated using flavour specific, self-tagging, decays.

The statistical uncertainty on C_f, S_f, and $S_{\overline{f}}$ scales with $1/\sqrt{\epsilon_{eff}}$, defined as $\epsilon_{eff} = \epsilon_{tag}(1-2\omega)^2$ where ϵ_{tag} is the efficiency to tag an event. Therefore, the tagging algorithms are tuned for maximum effective tagging power. The obtained tagging power is collected in Table 1.

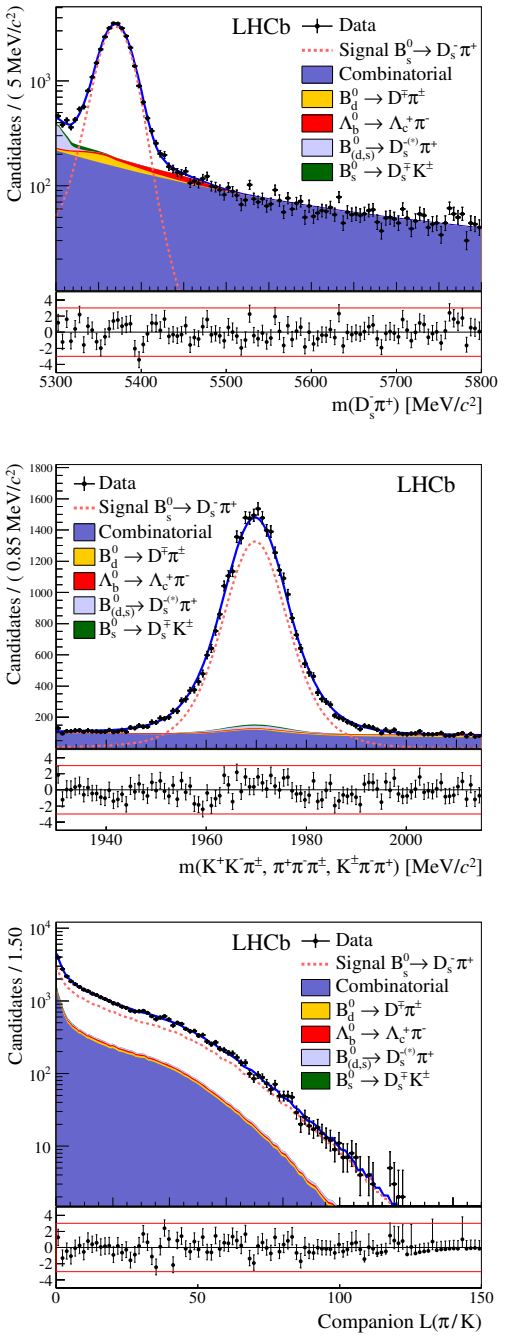

Figure 1: The multivariate fit to the $B_s^0 \to D_s^- \pi^+$ candidates for all D_s^- decay modes combined. From top to bottom: distributions of candidates in B_s^0 mass, D_s^- mass, companion PID log-likelihood difference.

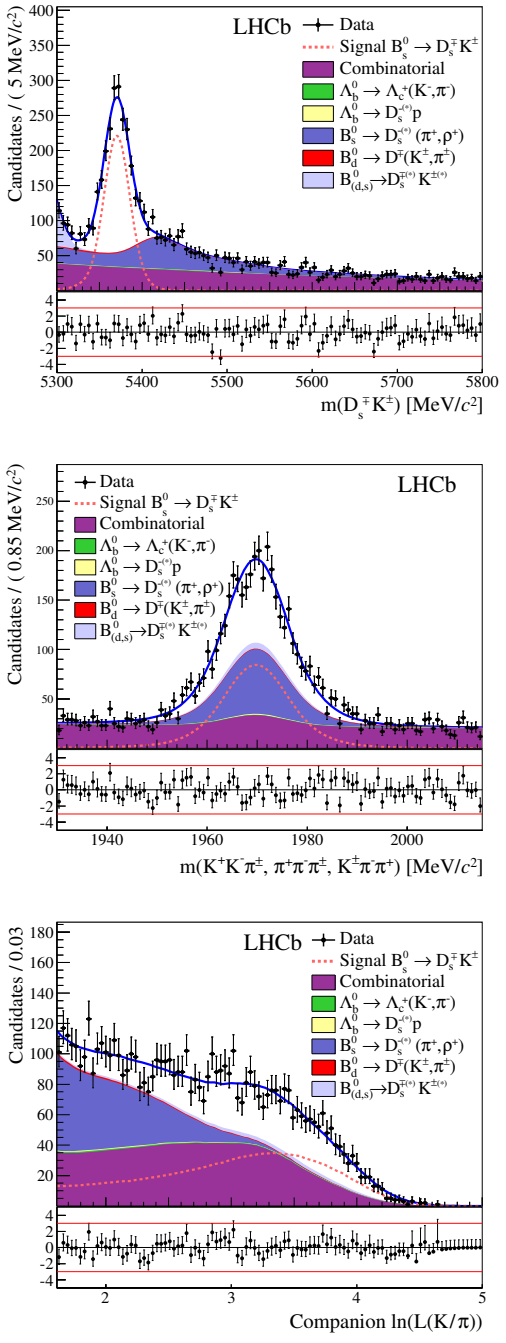

Figure 2: The multivariate fit to the $B_s^0 \to D_s^\mp K^\pm$ candidates for all D_s^- decay modes combined. From top to bottom: distributions of candidates in B_s^0 mass, D_s^- mass, companion PID log-likelihood difference.

Table 1: Flavour tagging performance for the three different tagging categories for $B_s^0 \to D_s^- \pi^+$ candidates.

Event type	ϵ_{tag} [%]	ϵ_{eff} [%]
OS-only	19.80 ± 0.23	1.61 ± 0.03 ± 0.08
SSK-only	28.85 ± 0.27	1.31 ± 0.22 ± 0.17
OS-SSK	18.88 ± 0.23	2.15 ± 0.05 ± 0.09
Total	67.53	5.07

4.2. Decay time resolution and acceptance

Due to fast $B_s^0 - \overline{B}_s^0$ oscillations the decay-time resolution of the detector has to be taken into account. The per-candidate decay-time uncertainty is used as an observable in the nominal fit. The calibration of the per-candidate decay-time uncertainty is required and performed using prompt D_s^- mesons combined with a random track and kinematically weighted to give a sample of "fake B_s^0" candidates. The scale factor is found to be 1.37 ± 0.10.

Non-negligible correlations between CP observables and the acceptance of the selection does not allow the latter to float in the nominal fit. The acceptance is fixed based on information from the $B_s^0 \to D_s^- \pi^+$ fit and corrected by the acceptance ratio of $B_s^0 \to D_s^\mp K^\pm$ and $B_s^0 \to D_s^- \pi^+$ found in simulation. In the above $B_s^0 \to D_s^- \pi^+$ fit Δm_s is floating, giving value of 17.772 ± 0.022 ps^{-1} which is in excellent agreement with the published LHCb measurement of $\Delta m_s = 17.768 \pm 0.023 \pm 0.006$ ps^{-1} [6]. The result of $B_s^0 \to D_s^- \pi^+$ fit is shown in Fig. 3.

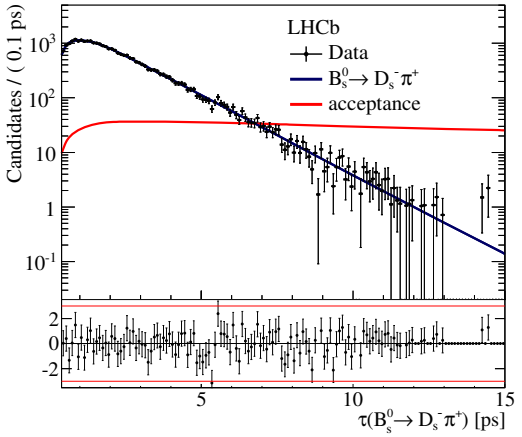

Figure 3: Result of the fit to the decay-time distribution of $B_s^0 \to D_s^- \pi^+$ candidates, which is used to measure the decay-time acceptance in $B_s^0 \to D_s^\mp K^\pm$ decays. The solid curve is the measured decay-time acceptance.

4.3. Time fits

The determination of the CP parameters is performed using an unbinned maximum likelihood fit in two different approaches: in one all signal and background time distributions are described (*cFit*), and in a second the background is statistically subtracted using the *sPlot* technique [7] where only the signal time distributions are described (*sFit*). The signal decay-time model is identical in the two fitters.

The following parameters are fixed from independent measurements [6, 8, 9]:
$\Gamma_s = (0.661 \pm 0.007) ps^{-1}$, $\Gamma_{\Lambda_b^0} = (0.676 \pm 0.006) ps^{-1}$,
$\Delta\Gamma_s = (0.106 \pm 0.013) ps^{-1}$, $\Gamma_d = (0.658 \pm 0.003) ps^{-1}$,
$\Delta m_s = (17.768 \pm 0.024) ps^{-1}$, $\rho(\Gamma_s, \Delta\Gamma_s) = -0.39$,
here $\rho(\Gamma_s, \Delta\Gamma_s)$ is the correlation between these two measurements, $\Gamma_{\Lambda_b^0}$ is the decay-width of the Λ_b^0 baryon, Γ_d is the B_d^0 decay width, and Δm_s is the B_s^0 oscillation frequency. The parameters corresponding to B_d^0 mesons or Λ_b^0 baryons are used only in the *cFit* case.

Decay-time PDFs for signal and background components contain the effects of flavour tagging, are convolved with a single Gaussian representing the per-candidate decay-time resolution, and are multiplied by the decay-time acceptance. In the *sFit* approach the signal $B_s^0 \to D_s^\mp K^\pm$ model is fitted to the *sWeighted* data sample, while the *cFit* performs a six-dimensional fit with full signal and background components description to: the decay time, decay-time uncertainty, predicted mistag, and the three variables used in the multivariate fit. In the case of *cFit*, the following assumptions are made: the B_s^0 mass range is restricted to be in $[5320, 5420]$ MeV/c^2 and the yields of the different signal and background components are fixed to those found in this fit range in the multivariate fit. The decay-time range of the both fits is $\tau(B_s^0) \in [0.4, 15.0]$ ps^{-1}. The results of the *cFit* and *sFit* for the CP violating observables are given in Table 2, and shown in Fig. 4.

Table 2: Fitted values of the CP observables to the $B_s^0 \to D_s^\mp K^\pm$ time distribution for (left) *sFit* and (right) *cFit*, where the first uncertainty is statistical, the second is systematic.

Parameter	sFit fitted value	cFit fitted value
C_f	0.52 ± 0.25 ± 0.04	0.53 ± 0.25 ± 0.04
S_f	−0.90 ± 0.31 ± 0.06	−1.09 ± 0.33 ± 0.08
$S_{\bar{f}}$	−0.36 ± 0.34 ± 0.06	−0.36 ± 0.34 ± 0.08
$A_f^{\Delta\Gamma}$	0.29 ± 0.42 ± 0.17	0.37 ± 0.42 ± 0.20
$A_{\bar{f}}^{\Delta\Gamma}$	0.14 ± 0.41 ± 0.18	0.20 ± 0.41 ± 0.20

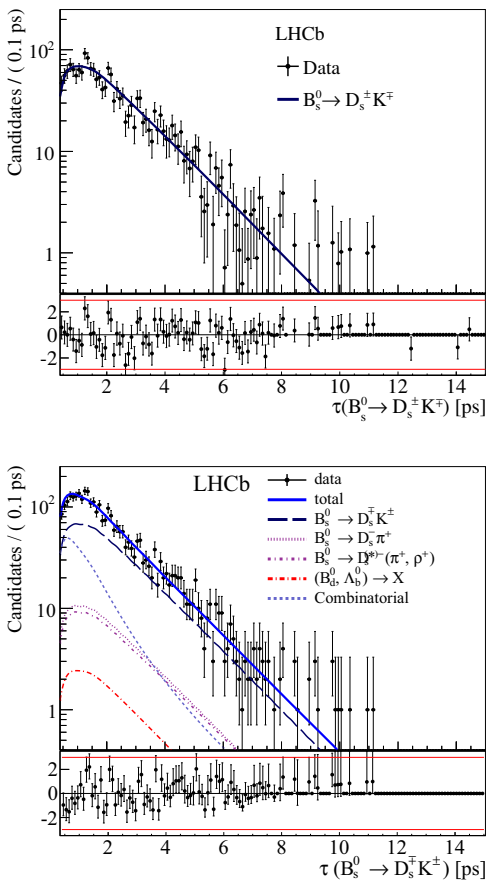

Figure 4: Result of the decay-time (top) *sFit* and (bottom) *cFit* to the $B_s^0 \to D_s^\mp K^\pm$ candidates.

4.4. Systematics

In the measurement the following sources of systematic uncertainties are found: uncertainties from the fixed parameters Δm_s, Γ_s, and $\Delta\Gamma_s$, uncertainties from the limited knowledge of the decay time resolution and acceptances and uncertainties from data splits. The first two are estimated using large sets of simulated pseudo-experiments, in which the relevant parameters are varied. The third is computed based on performed data splits.

Since the acceptance parameters are determined from the fit to $B_s^0 \to D_s^-\pi^+$ candidates, where Γ_s and $\Delta\Gamma_s$ are fixed, the systematic uncertainty on the acceptance is strongly anti-correlated with Γ_s and $\Delta\Gamma_s$. The correlations between them are taken into account and quoted together.

In addition, the cFit contains fixed parameters describing the decay time of the combinatorial background. These parameters are found to be correlated to the CP parameters, and a systematic uncertainty is assigned.

Table 3: Systematic uncertainties, relative to the statistical uncertainty, for *sFit*.

Parameter	C_f	$A_f^{\Delta\Gamma}$	$A_{\overline{f}}^{\Delta\Gamma}$	S_f	$S_{\overline{f}}$
Δm_s	0.062	0.013	0.013	0.104	0.100
scale factor	0.104	0.004	0.004	0.092	0.096
acceptance, Γ_s, $\Delta\Gamma_s$	0.043	0.427	0.437	0.039	0.038
sample splits	0.124	0.000	0.000	0.072	0.071
total	0.179	0.427	0.437	0.161	0.160

Table 4: Systematic uncertainties, relative to the statistical uncertainty, for *cFit*.

Parameter	C_f	$A_f^{\Delta\Gamma}$	$A_{\overline{f}}^{\Delta\Gamma}$	S_f	$S_{\overline{f}}$
Δm_s	0.068	0.014	0.011	0.131	0.126
scale factor	0.131	0.004	0.004	0.101	0.103
acceptance, Γ_s, $\Delta\Gamma_s$	0.050	0.461	0.464	0.050	0.043
comb. bkg. lifetime	0.016	0.069	0.072	0.015	0.005
sample splits	0.102	0.000	0.000	0.156	0.151
total	0.187	0.466	0.470	0.234	0.226

The summary of systematic uncertainties described as a fraction of statistical uncertainties are shown in Table 3 and Table 4 for *sFit* and *cFit*, respectively.

5. Determination of the CKM γ angle

The determination of the CKM angle γ is based on the *cFit* results which are arbitrarily chosen as nominal. The measurement of the CP-sensitive parameters is interpreted in terms of $\gamma - 2\beta_s$. The strategy is to maximise the following likelihood

$$\mathcal{L}(\vec{\alpha}) = exp(-\tfrac{1}{2}(\vec{A}(\vec{\alpha}) - \vec{A}_{obs})^T V^{-1}(\vec{A}(\vec{\alpha}) - \vec{A}_{obs})), \quad (5)$$

where $\vec{\alpha} = (\gamma, \phi_s, r_{D_sK}, \delta)$ is the vector of the physics parameters, $\vec{A}$ is the vector of observables, $\vec{A}_{obs}$ is the vector of the measured CP violating observables and V is the experimental (statistical and systematic) covariance matrix.

The value of mixing phase is constrained to $\phi_s = 0.01 \pm 0.07(stat) \pm 0.01(syst)$ *rad* from the LHCb measurement of $B_s^0 \to J/\phi K^+K^-$ and $B_s^0 \to J/\phi\pi^+\pi^-$ decays [9]. Since penguin pollution is neglected and no BSM contribution are expected in these decays it gives $\phi_s = -2\beta_s$.

Confidence intervals are computed using a frequentist method based on pseudo experiments, and found to be:

$$\gamma = (115^{+28}_{-43})^\circ,$$
$$\delta_{D_sK} = (3^{+19}_{-20})^\circ,$$
$$r_{D_sK} = 0.53^{+0.17}_{-0.16},$$

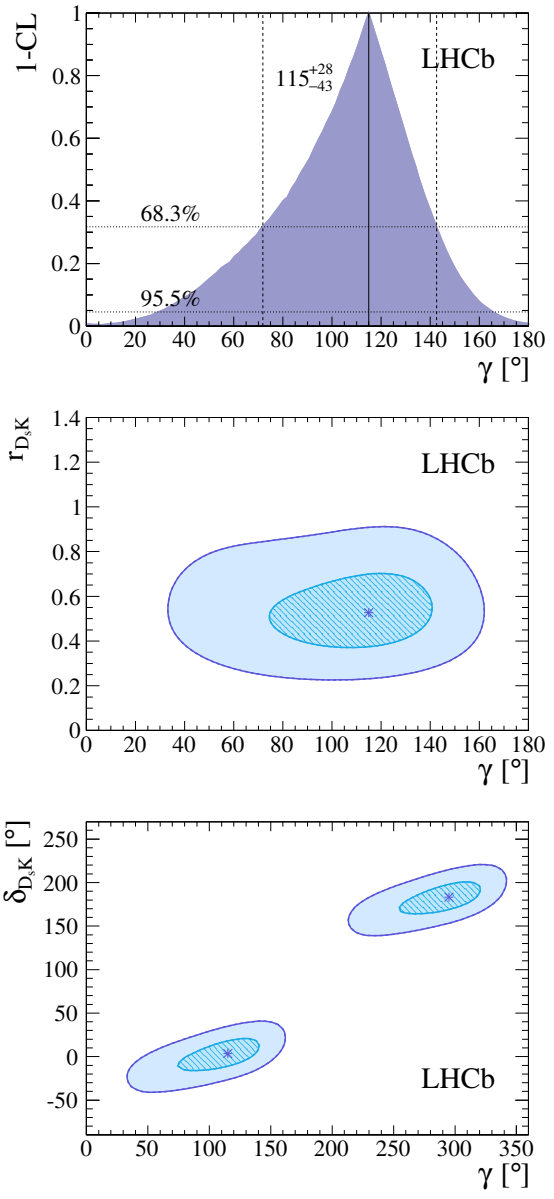

Figure 5: Graph showing 1-CL for γ, together with the central value and the 68.3% CL interval as obtained from the frequentist method described in the text (top). Profile likelihood contours of r_{D_sK} vs. γ (middle), and δ vs. γ (bottom). The contours are the 1σ (2σ) profile likelihood contours, corresponding to 39% CL (86% CL) in Gaussian approximation. The markers denote the best-fit values.

where the intervals for the angles are expressed modulo 180°. Figure 5 shows the 1 − CL curve for γ, and the two-dimensional contours of the profile likelihood.

6. Conclusion

The CP violation sensitive parameters from $B_s^0 \to D_s^{\mp}K^{\pm}$ decays have been measured using a dataset of 1.0 fb^{-1} of pp collision data. Their values are found to be

$$\begin{aligned} C_f &= \ 0.53 \pm 0.25 \pm 0.04, \\ A_f^{\Delta\Gamma} &= \ 0.37 \pm 0.42 \pm 0.20, \\ A_{\overline{f}}^{\Delta\Gamma} &= \ 0.20 \pm 0.41 \pm 0.20, \\ S_f &= -1.09 \pm 0.33 \pm 0.08 \\ S_{\overline{f}} &= -0.36 \pm 0.34 \pm 0.08, \end{aligned}$$

where the first uncertainties are statistical and the second are systematic. The results are interpreted in terms of the CKM angle γ, which is found to be $\gamma = (115^{+28}_{-43})^\circ$ modulo 180° at the 68% confidence level. This is the world-first measurement of γ performed from $B_s^0 \to D_s^{\mp}K^{\pm}$ decays.

Acknowledgments

I would like to thank polish National Science Center for partially financing research and fully financing my attendance of the conference (DEC-2012/07/N/ST2/02890, DEC-2013/08/T/ST2/00035). This research was also supported in part by PL-Grid Infrastructure.

References

[1] N. Cabibbo, Unitary symmetry and leptonic decays, Phys. Rev. Lett. 10 (1963) 531.
[2] M. Kobayashi and T. Maskawa, CP violation in the renormalizable theory of weak interaction, Prog. Theor. Phys. 49 (1973) 652.
[3] R. Fleischer, New strategies to obtain insights into CP violation through $B_{(s)} \to D_{(s)}^{\pm}K^{\mp}, D_{(s)}^{*\pm}K^{\mp}$, ... $B_{(d)} \to D^{\pm}\pi^{\mp}, D^{*\pm}\pi^{\mp}$, ... decays, Nucl. Phys. B671 (2003) 459.
[4] LHCb collaboration, A. A. Alves Jr. et al., The LHCb detector at the LHC, JINST 3 (2008) S08005.
[5] M.Dorigo, b-flavour tagging in pp collisions, this proceedings.
[6] LHCb collaboration, R. Aaij et al., Precision measurement of the $B_s^0 - \overline{B}_s^0$ oscillation frequency in the decay $B_s^0 \to D_s^-\pi^+$, New J. Phys. 15 (2013) 053021,
[7] M. Pivk and F. R. Le Diberder, sPlot: a statistical tool to unfold data distributions, Nucl. Instrum. Meth. A555 (2005) 356.
[8] Particle Data Group, J. Beringer et al., Review of particle physics, Phys. Rev. D86 (2012) 010001.
[9] LHCb collaboration, R. Aaij et al., Measurement of CP violation and the B_s^0 meson decay width difference with $B_s^0 \to J/\phi K^+K^-$ and $B_s^0 \to J/\phi\pi^+\pi^-$ decays, Phys. Rev. D87 (2013) 112010.
[10] LHCb collaboration, R. Aaij et al., A measurement of the CKM angle γ from a combination of $B^{\pm} \to Dh^{\pm}$ analyses, Phys. Lett. B726 (2013)